

Model-independent cosmological constraints from growth and expansion

Benjamin L’Huillier,^{1*} Arman Shafieloo,^{1,2} and Hyungjin Kim³

¹*Korea Astronomy and Space Science Institute, Yuseong-gu, 776 Daedeok daero, Daejeon 34055, Korea*

²*University of Science and Technology, Yuseong-gu 217 Gajeong-ro, Daejeon 34113, Korea*

³*Department of Applied Mathematics, University of Waterloo, Waterloo, Ontario, N2L 3G1, Canada*

Accepted February 6, 2018. Received February 4, 2018; in original form January 3, 2018

ABSTRACT

Reconstructing the expansion history of the Universe from type Ia supernovae data, we fit the growth rate measurements and put model-independent constraints on some key cosmological parameters, namely, Ω_m , γ , and σ_8 . The constraints are consistent with those from the concordance model within the framework of general relativity, but the current quality of the data is not sufficient to rule out modified gravity models. Adding the condition that dark energy density should be positive at all redshifts, independently of its equation of state, further constrains the parameters and interestingly supports the concordance model.

Key words: cosmology: theory – large-scale structure of universe – methods: numerical – methods: statistical

1 INTRODUCTION

The discovery of the acceleration of the expansion of the Universe (Riess et al. 1998; Perlmutter et al. 1999) led to the emergence of the Λ CDM paradigm, further supported by the study of the cosmological microwave background (Bennett et al. 2003; Planck Collaboration XIII 2016) and the large-scale structures of the Universe (e.g., Eisenstein et al. 2005; Alam et al. 2017). In this paradigm, gravity is described by general relativity (GR), and the energy budget is dominated by the cosmological constant as dark energy (DE), responsible for the acceleration of the expansion, and a smooth, cold dark matter component. However, the nature of DE is one of the biggest mysteries of modern physics, and the simplest candidate, the cosmological constant, poses theoretical problems (e.g., Weinberg 1989; Peebles & Ratra 2003). Alternatively, general relativity may not be the correct theory to describe gravity, and the acceleration may reflect departure from GR.

At the background level, for a flat universe, the expansion of the smooth Universe $h(z) = H(z)/H_0$ follows

$$h^2(z) = \Omega_m(1+z)^3 + \Omega_{\text{DE}}(z), \quad (1)$$

where H_0 is the Hubble constant today, Ω_m the matter

energy density today,

$$\Omega_{\text{DE}}(z) = (1 - \Omega_m) \exp\left(3 \int_0^z \frac{1+w(z')}{1+z'} dz'\right), \quad (2)$$

the DE contribution to the energy density, and $w(z) = P_{\text{DE}}/\rho_{\text{DE}}$ is the DE equation of state. For a cosmological constant Λ , $w \equiv -1$ and $\Omega_{\text{DE}}(z) = \Omega_\Lambda \equiv 1 - \Omega_m$, but current data do not rule out models such as quintessence or dynamical DE models (e.g. Ooba et al. 2017; Zhao et al. 2017).

Meanwhile, at the perturbation level, the growth rate f is defined as

$$f(z) = \frac{d \ln \delta}{d \ln a} \simeq \Omega_m^\gamma(z), \quad (3)$$

where γ is the growth index (Linder 2005; Linder & Cahn 2007; Linder 2017), and

$$\Omega_m(z) = \frac{\Omega_m(1+z)^3}{h^2(z)} \quad (4)$$

is the matter contribution to the energy density at a given redshift.

Observationally, redshift-space distortion measures

$$f\sigma_8(z) \simeq \sigma_8(0)\Omega_m^\gamma(z) \exp\left(-\int_0^z \Omega_m^\gamma(z') \frac{dz'}{1+z'}\right), \quad (5)$$

where $\sigma_8^2(z)$ is the mass variance in a $8 h^{-1}$ Mpc sphere. For simplicity, we will denote $\sigma_8 = \sigma_8(0)$ when there is no ambiguity.

* E-mail: benjamin@kasi.re.kr, shafieloo@kasi.re.kr

From eq. (4) and (5), it is clear that $f\sigma_8$ depends on $(\Omega_m, \gamma, \sigma_8)$ as well as the expansion history $h(z)$. In general relativity (GR), $\gamma \simeq 0.55$, while modified theories of gravity such as $f(R)$ (de Felice & Tsujikawa 2010) or DGP (Dvali et al. 2000) predict different (possibly scale-dependent) values of γ (Linder & Cahn 2007). Therefore, $f\sigma_8$ is a powerful probe of gravity. Moreover, joined measurements of $h(z)$ and $f\sigma_8$ can help break degeneracies between modified gravity theories and dark energy (Linder 2005, 2017). Therefore, it has been used to test the Λ CDM model or alternative gravities theories (e.g., Nesseris & Perivolaropoulos 2008; Bean & Tangmatitham 2010; Basilakos 2012; Shafieloo et al. 2013; Gómez-Valent et al. 2015; Ruiz & Huterer 2015; Mueller et al. 2016; Nesseris et al. 2017; Solà et al. 2017).

In this paper, we aim to constrain some key cosmological parameters, namely, Ω_m, σ_8 , and γ , by fitting the growth data using model-independent expansion histories that do not assume any DE model.

§ 2 describes the data and method, our results are shown in § 3. § 4 explores the effects of restricting the DE density to be positive at all redshift, and our conclusions are drawn in § 5.

2 METHOD

We used reconstructed expansion histories from the Joint Lightcurve Analysis (JLA, Betoule et al. 2014) and combined them with growth measurements.

2.1 Model-independent reconstructions of the expansion history

We reconstructed the expansion history from the JLA compilation (unbinned data with full covariance matrix) using the iterative model-independent smoothing method (Shafieloo et al. 2006; Shafieloo 2007; L’Huillier & Shafieloo 2017). Starting from some initial guess $\hat{\mu}_0(z)$, we calculate the smooth distance modulus at any redshift z at iteration $n+1$ as

$$\hat{\mu}_{n+1}(z) = \hat{\mu}_n(z) + N(z) \sum_i \frac{\mu(z_i) - \hat{\mu}_n(z_i)}{\sigma_i^2} \exp\left(-\frac{\ln^2\left(\frac{1+z_i}{1+z}\right)}{2\Delta^2}\right), \quad (6)$$

where

$$N^{-1}(z) = \sum_i \frac{1}{\sigma_i^2} \exp\left(-\frac{\ln^2\left(\frac{1+z_i}{1+z}\right)}{2\Delta^2}\right) \quad (7)$$

is a normalization factor, $\mu(z_i)$ and σ_i are the measured distance modulus and its associated error at redshift z_i , and $\Delta = 0.3$ is the smoothing length.

We then obtain the smooth luminosity distances

$$d_L(z) = 10^{\mu/5-5} \text{Mpc}. \quad (8)$$

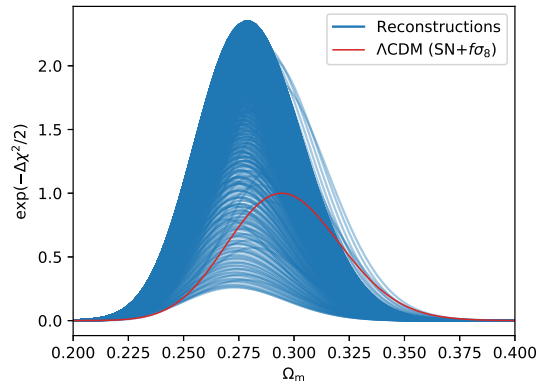


Figure 1. $\exp(-\Delta\chi^2/2)$ (with respect to the best-fit Λ CDM model) versus Ω_m for each reconstruction, fixing $(\gamma, \sigma_8) = (0.55, 0.80)$. The red line shows the Λ CDM case.

Assuming a flat universe, we can calculate

$$h(z) = \frac{c}{H_0} \left[\frac{d}{dz} \left(\frac{d_L(z)}{1+z} \right) \right]^{-1}. \quad (9)$$

Varying the initial guess $\hat{\mu}_0$, we end up with few thousands reconstructions and calculate their χ^2 as

$$\chi_{\text{SN},n}^2 = \delta\mu_n^T \mathbf{C}^{-1} \delta\mu_n, \quad (10)$$

where

$$\delta\mu_n = \hat{\mu}_n - \mu_i \quad (11)$$

is the residual vector for a given reconstruction n and \mathbf{C} is the covariance matrix provided by Betoule et al. (2014). We then only keep reconstructions such that $\chi_{\text{SN},n}^2 < \chi_{\text{SN},\Lambda\text{CDM}}^2$. These reconstructions represent a non-exhaustive sample of plausible expansion histories.

We should note that the method of smoothing we used in this work is in fact insensitive to the initial conditions and choice of the smoothing scale (c.f. Shafieloo et al. 2006; Shafieloo 2007): whatever the initial conditions, the method converges to the solution preferred by the data. However, they will approach this final solution via different paths. The central idea of using the iterative smoothing in this work is to come with a *non-exhaustive* sample of plausible expansion histories of the Universe directly reconstructed from the data, therefore we start the procedure with several initial conditions and combine the results at the end.

2.2 Combining the likelihoods

For each reconstructed $h_n(z)$, we can calculate $f\sigma_8$ for some $(\Omega_m, \gamma, \sigma_8)$ by computing the integral in eq. (5). We can thus explore the parameter space, and compare to growth measurements to obtain a χ^2 for the growth data. We used a compilation of growth data points from 2dFGRS (Song & Percival 2009), WiggleZ (Blake et al. 2011), 6dFGRS (Beutler et al. 2012), the VIPERS (de la Torre & Peacock 2013), the SDSS

Main galaxy sample (Howlett et al. 2015), 2MTF (Howlett et al. 2017), and BOSS DR12 (Gil-Marín et al. 2017). We did not include the FastSound data (Okumura et al. 2016) at $z = 1.4$, since our smooth reconstructions do not reach that redshift.

Since both datasets are independent, we can multiply the likelihood, or equivalently sum the χ^2 . Since the growth data are mutually independent, their χ^2 is simply defined as

$$\chi_{f\sigma_8}^2 = \sum_i \left(\frac{f\hat{\sigma}_8(z_i|\gamma, \Omega_m, \sigma_8) - f\sigma_{8,i}}{\sigma_{f\sigma_{8,i}}} \right)^2. \quad (12)$$

The total χ_n^2 for reconstruction n is thus $\chi_n^2 = \chi_{\text{SN},n}^2 + \chi_{f\sigma_{8,n}}^2$. We can then find the parameters that minimize the χ^2 , and their associated confidence intervals.

3 RESULTS

Using the reconstructed expansion histories $h(z)$, we calculate the χ^2 as defined in § 2.2. First, we fixed $(\gamma, \sigma_8) = (0.55, 0.80)$, and allow Ω_m to vary. Since the reconstructed $h(z)$ were obtained assuming a flat universe, Ω_m is allowed to vary between 0 and 1. For reference, we calculate the χ^2 of the Λ CDM model, and find its minimum $\chi_{\text{min},\Lambda\text{CDM}}^2$. We are interested in $\Delta\chi^2 = \chi^2 - \chi_{\text{min},\Lambda\text{CDM}}^2$, the difference with respect to the best-fit Λ CDM case. Fig. 1 shows $\mathcal{L} = \exp(-\Delta\chi^2/2)$ as a function of Ω_m for each reconstruction (in blue). Therefore, combinations of h and Ω_m with a better χ^2 than the best-fit Λ CDM model ($\Delta\chi^2 < 0$), have a likelihood larger than one. For comparison, we also show in red $\mathcal{L}_{\Lambda\text{CDM}} = \exp(-\Delta\chi^2/2)$ for the Λ CDM case. The model-independent reconstructions seem to favour slightly lower Ω_m with respect to the Λ CDM case. However, they are fully consistent with the Λ CDM case.

We then allow γ or σ_8 to vary together with Ω_m , while fixing the third parameter to its fiducial value ($\sigma_8 = 0.80$ or $\gamma = 0.55$). In both cases, we calculate χ^2 for the Λ CDM case, and find the regions where $\Delta\chi^2 < 2.3$ and $\Delta\chi^2 < 6.18$, corresponding to 1σ and 2σ for two degrees of freedom. Fig. 2 shows in red the 1σ and 2σ regions of the Λ CDM case. For each model-independent reconstruction, we then calculate the χ^2 of the model-independent case, and find the regions in the (σ_8, Ω_m) and (γ, Ω_m) planes where the reconstruction give a better χ^2 than the best-fit Λ CDM, namely, $\Delta\chi^2 < 0$. Fig. 2 shows in blue the superposition of these regions over all reconstructions in the (Ω_m, σ_8) (left) and (Ω_m, γ) (right) planes. Therefore, if a point (σ_8, Ω_m) (or (γ, Ω_m)) is located in the blue region, there exists at least one reconstruction that, combined with (σ_8, Ω_m) (or (γ, Ω_m)), yields a better χ^2 than the best-fit Λ CDM model.

Fixing $\gamma = 0.55$ yields higher preferred values for Ω_m , while fixing $\sigma_8 = 0.80$ yields lower preferred values. However, the model-independent approach is fully consistent with Λ CDM. Moreover, it can be seen

that, when $h(z)$ is not restricted to Λ CDM, there is a stronger degeneracy in the parameters. Namely, it is possible to find expansions histories that, coupled with low values of Ω_m and γ , or with high values of Ω_m and σ_8 , give a better fit to the combined data. The degeneracy in the parameters can be understood from eq. 5: for fixed σ_8 , Ω_m^γ should stay roughly constant, therefore lower Ω_m are compensated by lower γ . Similarly, for fixed γ , $\Omega_m\sigma_8$ should stay constant, therefore lower Ω_m demand higher σ_8 . This is consistent with the results of Shafieloo et al. (2013), with slightly tighter constraints.

Finally, we vary all three parameters $(\Omega_m, \gamma, \sigma_8)$ simultaneously. Fig. 3 shows in red the projections of the $\Delta\chi^2 < 3.53$ and 8.02 regions of the Λ CDM case, corresponding to 1σ and 2σ for three degrees of freedom, onto the (σ_8, γ) (top-left), (σ_8, Ω_m) (bottom-left), and (γ, Ω_m) (bottom-right). For the model-independent case, we proceed as in Fig. 2, and find the $\Delta\chi^2 < 0$ regions for each reconstruction. We then show in blue the projection onto the three planes of the superposition of the $\Delta\chi^2 < 0$ regions over all reconstruction. Again, the blue region shows the region of the parameter-space where there is at least one model-independent reconstruction that yields a better χ^2 than the best-fit Λ CDM model.

The model-independent joint constraints on $(\Omega_m, \gamma, \sigma_8)$ are now very broad. They are fully consistent with the Λ CDM model. The $\Delta\chi^2 < 0$ region is consistent with both $\Omega_m = 0$ and $\Omega_m = 1$, while it allows γ between about 0.1 and 1, and σ_8 between 0.25 and 1.25.

4 DARK ENERGY CONSTRAINTS

In the previous section, we considered all combinations of $(\Omega_m, h(z))$, with the only restriction $\Omega_m < 1$, since the $h(z)$ were obtained assuming a flat universe. Rewriting equation (2) as

$$\Omega_{\text{de}}(z) = h^2(z) - \Omega_m(1+z)^3, \quad (13)$$

another constraint arises. Namely, the equation of state w is well defined, i.e., does not have a singularity, if $\Omega_{\text{DE}}(z) > 0$ at all redshift.

Therefore, even though some models can have negative DE density (Sahni & Shtanov 2003; Sahni et al. 2014, e.g.), in this section, we only consider combinations of $h(z)$ and Ω_m respecting the positivity condition

$$h^2(z) - \Omega_m(1+z)^3 \geq 0 \quad (14)$$

for all z .

We can then use this to reconstruct the dark energy equation of state

$$\begin{aligned} w_{\text{de}}(z) &= \frac{\frac{2}{3}(1+z)\frac{h'(z)}{h(z)} - 1}{1 - \Omega_m(1+z)^3 h^{-2}} \\ &= \frac{1}{3} \frac{2q - 1}{1 - \Omega_m(z)}, \end{aligned} \quad (15)$$

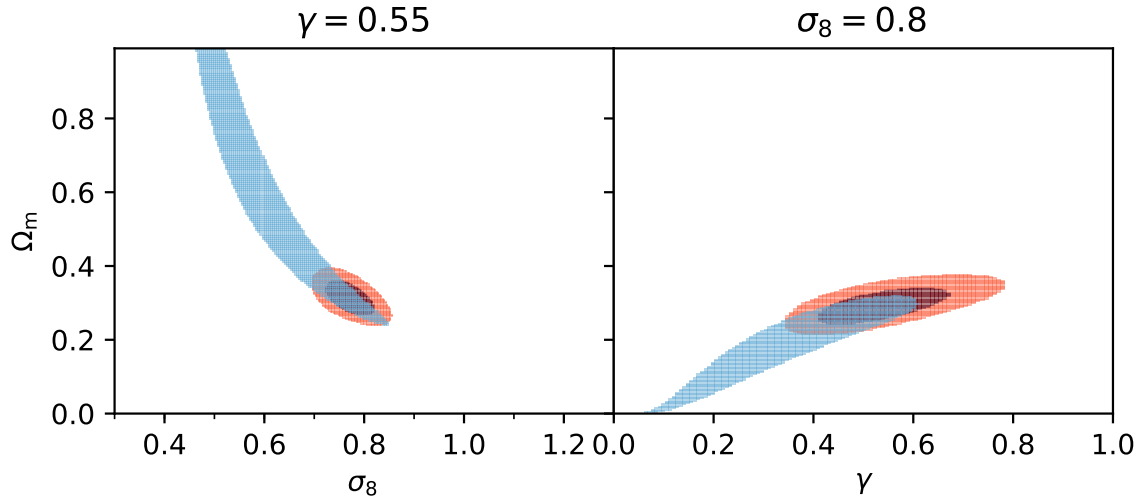


Figure 2. Superposition of the $\Delta\chi^2 < 0$ (with respect to the best-fit Λ CDM model) regions for $\gamma = 0.55$ (left) and $\sigma_8 = 0.80$ (right) in the model-independent case in blue. We also show in red the 1σ and 2σ regions of the Λ CDM model.

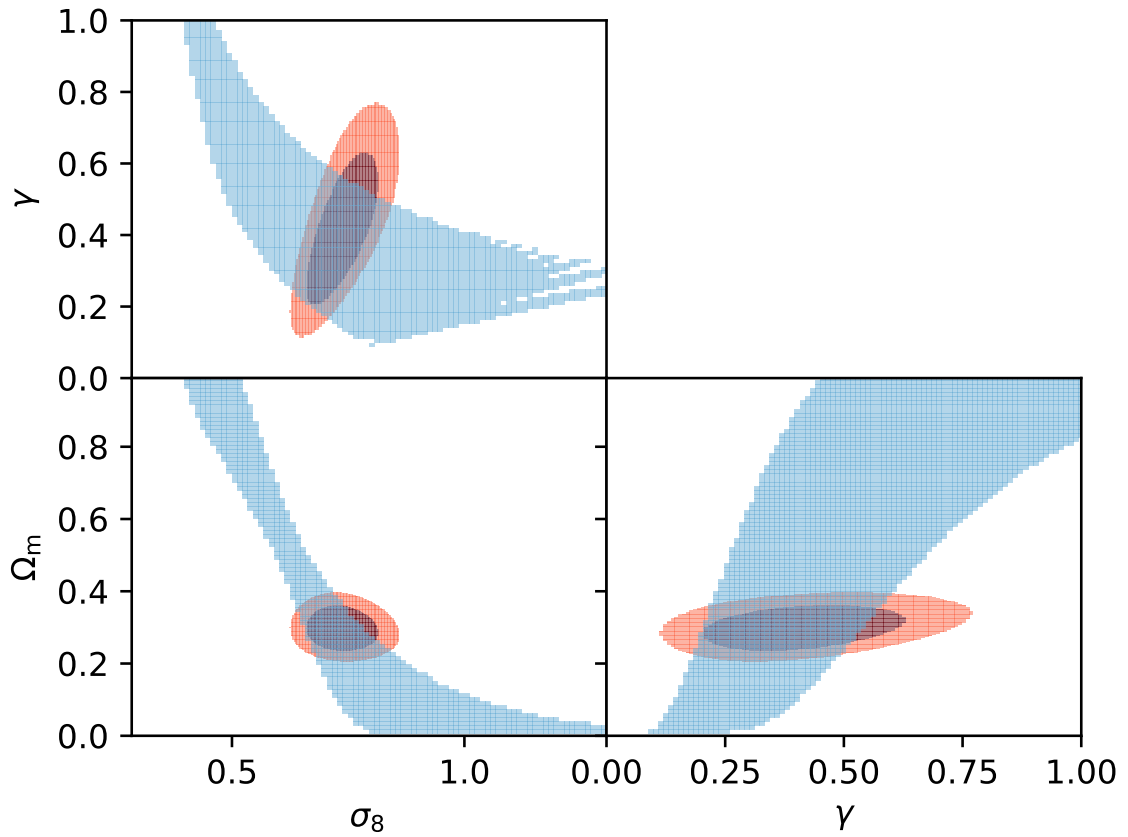


Figure 3. Superposition of the $\Delta\chi^2 < 0$ (with respect to the best-fit Λ CDM model) regions for $(\Omega_m, \gamma, \sigma_8)$ for the model-independent case (blue). In red we show the 1σ and 2σ regions for the Λ CDM case.

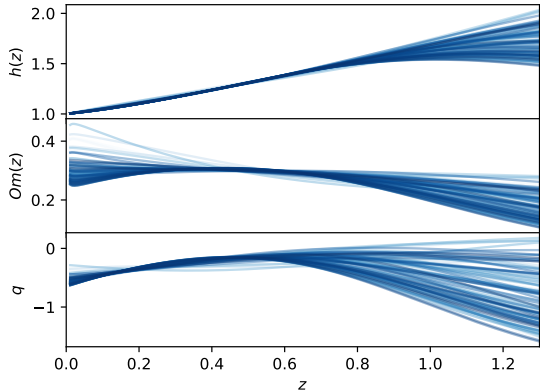


Figure 4. Reconstructed $h(z)$, $Om(z)$, and $q(z)$. The colour-code shows the index of the reconstruction.

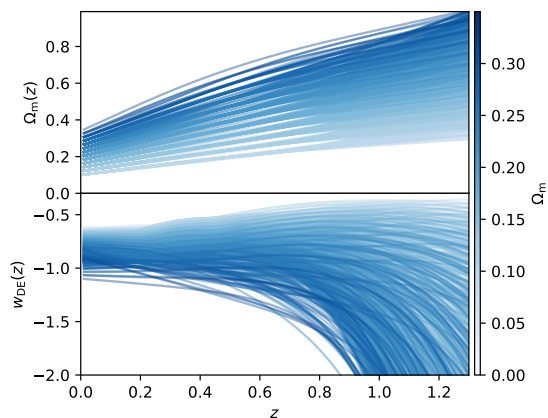


Figure 5. Reconstructed $\Omega_m(z)$ (top) and $w(z)$ (bottom) for different Ω_m and $h(z)$. All lines here verify eq. (14).

where

$$q(z) = (1+z) \frac{h'(z)}{h(z)} - 1 \quad (16)$$

is the deceleration parameter.

The top-, middle-, and bottom panels of Fig. 4 show the expansion history $h(z)$, the Om parameter (Sahni et al. 2008)

$$Om(z) = \frac{h^2(z) - 1}{(1+z)^3 - 1}, \quad (17)$$

and the deceleration parameter $q(z)$ for a random choice of about 5% of the reconstructions. For a flat Λ CDM Universe, $Om(z) \equiv \Omega_m$, thus Om is a litmus test for flat Λ CDM.

The top and bottom panels of Fig. 5 respectively show the matter density $\Omega_m(z)$ and the equation of state of DE for some combination of $(\Omega_m, h(z))$ verifying the positivity condition (14), colour-coded by the index of the reconstruction. The expansion histories that are closer from Λ CDM have a Om parameter close to constant, and their $q(z)$ can cross 0, while some reconstructions further from Λ CDM do not cross 0. When $\Omega_m(z)$ crosses 1, eq. (14) ceases to be valid, therefore none of the lines shown here crosses 1.

We can now add the positivity condition (14) as a hard prior on Ω_m in the previous analysis. Indeed, large values of Ω_m combined with some reconstructions can lead to negative DE density, and these combinations should thus be rejected. Figs. 6 and 7 show in blue the superposition over all reconstructions verifying equation (14) of the projected $\Delta\chi^2 < 0$ regions of the parameter space. The red contours are unchanged with respect to Figs 2 and 3.

In Fig. 6, while the $\sigma_8 = 0.8$ case (right-hand panel) is not affected much, since it preferred lower values of Ω_m , the allowed region for the $\gamma = 0.55$ case is drastically reduced, and only a small space of the original $\Delta\chi^2 < 0$ regions (that is, before applying eq. (14)) is allowed. This region is located in the 2σ region of the Λ CDM case.

In Fig. 7, the $\Delta\chi^2 < 0$ regions in each projection are also truncated with respect to Fig. 3, restricting the lower range of σ_8 and the higher range of γ and Ω_m .

The positivity condition (14) is thus a very strong constraint on the cosmological parameters, since it forbids large values of $\Omega_m \gtrsim 0.4$. Indeed, for these values, the DE density crosses zero within our data range, therefore these values are not allowed here. On the other hand, for low enough values, $\Omega_{DE}(z)$ never crosses zero.

5 DISCUSSION AND CONCLUSION

Using model-independent reconstructions of the expansion history from type Ia supernovae data, we fit the growth data and obtain constraints on $(\Omega_m, \gamma, \sigma_8)$. These model-independent constraints on the cosmological parameters are broader than the Λ CDM ones, but fully consistent. When all three cosmological parameter are let free, they are not well constrained, and it is possible to find expansion histories with cosmological parameters that are far from the Λ CDM constraints that give a reasonable fit to the data.

However, when restricting the combinations of Ω_m and the reconstructed expansion histories $h(z)$ that yield a positive dark energy density parameter ($h^2(z) - \Omega_m(1+z)^3 > 0$), the constraints on the cosmological parameters become stronger. Moreover, when imposing GR, i.e., fixing $\gamma = 0.55$, the model-independent contours are truncated and fully contained within the Λ CDM ones, showing strong evidence in favour of Λ CDM. That is, combinations of large Ω_m with expansion histories that are too different from Λ CDM are excluded. It should be noted that in Linder (2005), γ depends on w following $\gamma(w) = 0.55 + 0.05w(z=1)$, therefore fixing $\gamma = 0.55$ is not completely model-independent. However, we expect it to have little influence on the results presented here.

Our constraints are more stringent than Shafieloo et al. (2013) thanks to the better quality of the data and the introduction of the DE density positivity condition. The results are consistent with a flat- Λ CDM

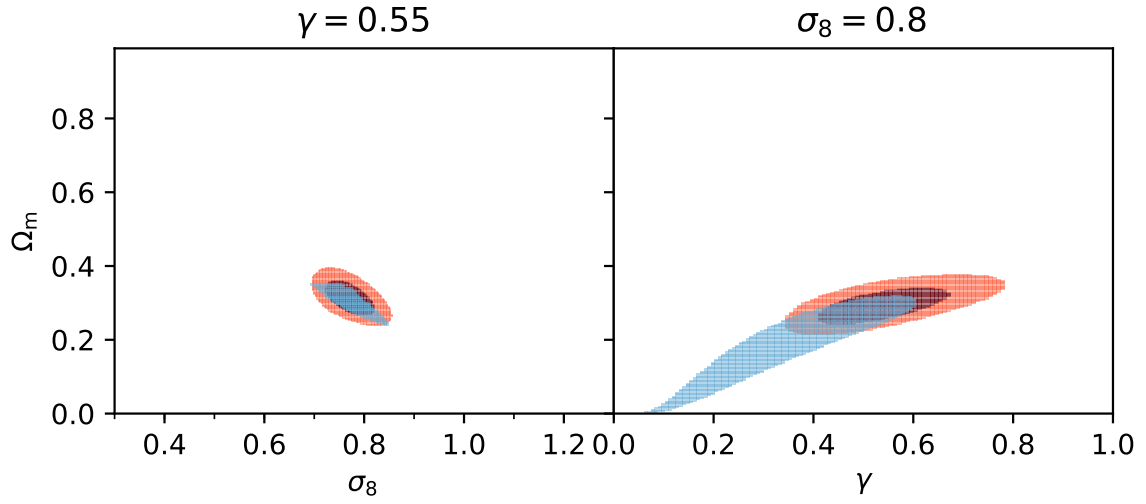


Figure 6. Blue: Truncation of the $\Delta\chi^2 < 0$ (with respect to the best-fit Λ CDM model) regions for $\gamma = 0.55$ (left) and $\sigma_8 = 0.80$ (right) in the model-independent case using eq. (14) as a hard prior. Red: 1σ and 2σ regions of the Λ CDM model.

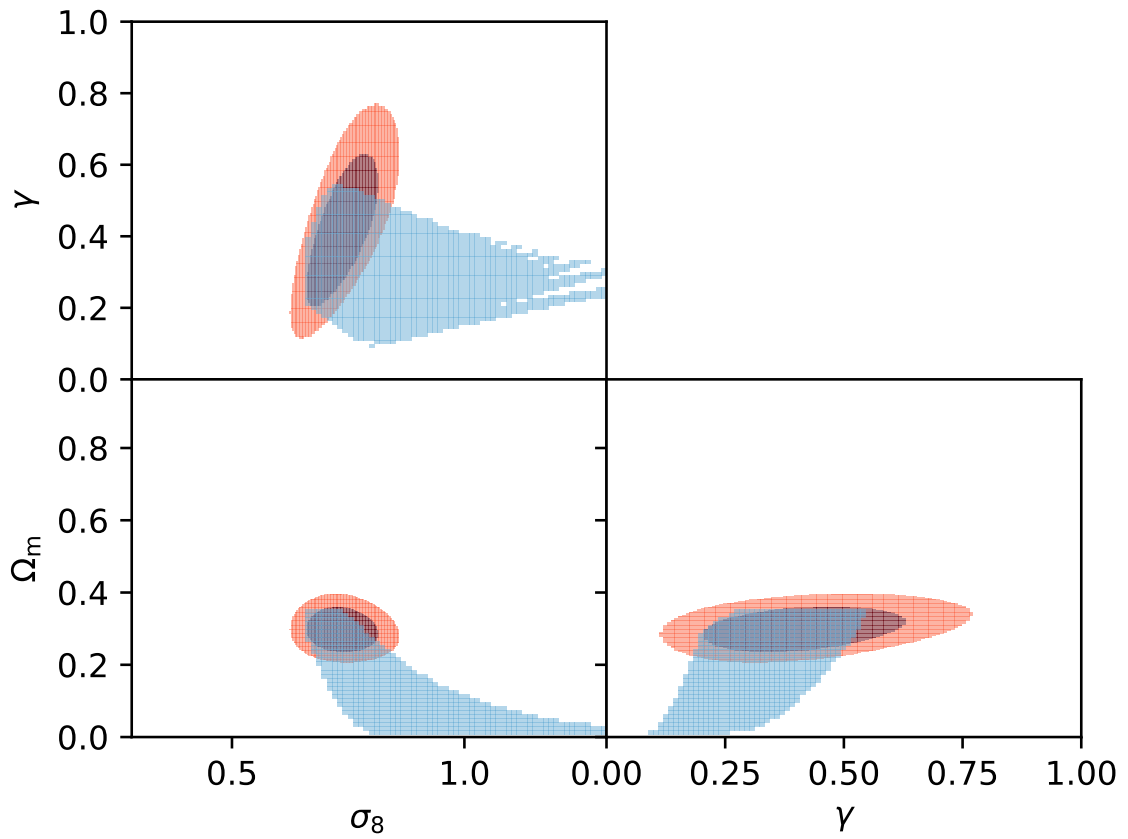


Figure 7. Blue: Truncation of the $\Delta\chi^2 < 0$ (with respect to the best-fit Λ CDM model) regions for $(\Omega_m, \gamma, \sigma_8)$ for the model-independent case using eq. (14) as a hard prior. Red: 1σ and 2σ regions of the Λ CDM case.

Universe and gravity described by general relativity, although modified theories of gravity predicting different growth index cannot be ruled out at this stage. The combined χ^2 being currently dominated by the supernovae data, better growth measurements are needed to further constrain gravity theory.

Future surveys such as the Dark Energy Spectroscopic Instrument (DESI Collaboration et al. 2016) will bring down the errors on the growth measurements, while surveys such as the Wide Field Infrared Survey Telescope (WFIRST, Spergel et al. 2015) and the Large Synoptic Survey Telescope (LSST, Ivezić et al. 2008) are expected to observe thousands of supernovae, increasing the quality of the data and covering a larger redshift range.

ACKNOWLEDGEMENTS

We thank Eric Linder for useful discussions, and Teppei Okumura for providing us with the $f\sigma_8$ data. The computations were performed by using the high performance computing cluster Polaris at the Korea Astronomy and Space Science Institute. A.S. would like to acknowledge the support of the National Research Foundation of Korea (NRF-2016R1C1B2016478). The authors thank the Yukawa Institute for Theoretical Physics at Kyoto University. Discussions during the CosKASI-ICG-NAOC-YITP joint workshop YITP-T-17-03 were useful to complete this work.

REFERENCES

- Alam S., et al., 2017, *MNRAS*, **470**, 2617
 Basilakos S., 2012, *International Journal of Modern Physics D*, **21**, 1250064
 Bean R., Tangmatitham M., 2010, *Phys. Rev. D*, **81**, 083534
 Bennett C. L., et al., 2003, *ApJS*, **148**, 1
 Betoule M., et al., 2014, *A&A*, **568**, A22
 Beutler F., et al., 2012, *MNRAS*, **423**, 3430
 Blake C., et al., 2011, *MNRAS*, **415**, 2876
 DESI Collaboration et al., 2016, preprint, ([arXiv:1611.00036](https://arxiv.org/abs/1611.00036))
 Dvali G., Gabadadze G., Porrati M., 2000, *Physics Letters B*, **485**, 208
 Eisenstein D. J., et al., 2005, *ApJ*, **633**, 560
 Gil-Marín H., Percival W. J., Verde L., Brownstein J. R., Chuang C.-H., Kitaura F.-S., Rodríguez-Torres S. A., Olmstead M. D., 2017, *MNRAS*, **465**, 1757
 Gómez-Valent A., Solà J., Basilakos S., 2015, *J. Cosmology Astropart. Phys.*, **1**, 004
 Howlett C., Ross A. J., Samushia L., Percival W. J., Manera M., 2015, *MNRAS*, **449**, 848
 Howlett C., et al., 2017, *MNRAS*, **471**, 3135
 Ivezić Z., et al., 2008, preprint, ([arXiv:0805.2366](https://arxiv.org/abs/0805.2366))
 L’Huillier B., Shafieloo A., 2017, *J. Cosmology Astropart. Phys.*, **1**, 015
 Linder E. V., 2005, *Phys. Rev. D*, **72**, 043529
 Linder E. V., 2017, *Astroparticle Physics*, **86**, 41
 Linder E. V., Cahn R. N., 2007, *Astroparticle Physics*, **28**, 481

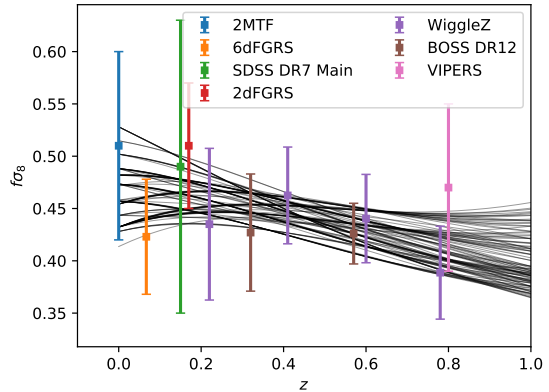


Figure A1. $f\sigma_8$ data and reconstructed $f\sigma_8$ with free ($\Omega_m, \gamma, \sigma_8$). All lines shown here have $\chi^2 < \chi^2_{\Lambda\text{CDM}}$.

- Mueller E.-M., Percival W., Linder E., Alam S., Zhao G.-B., Sánchez A. G., Beutler F., 2016, preprint, ([arXiv:1612.00812](https://arxiv.org/abs/1612.00812))
 Nesseris S., Perivolaropoulos L., 2008, *Phys. Rev. D*, **77**, 023504
 Nesseris S., Pantazis G., Perivolaropoulos L., 2017, *Phys. Rev. D*, **96**, 023542
 Okumura T., et al., 2016, *PASJ*, **68**, 38
 Ooba J., Ratra B., Sugiyama N., 2017, preprint, ([arXiv:1710.03271](https://arxiv.org/abs/1710.03271))
 Peebles P. J., Ratra B., 2003, *Reviews of Modern Physics*, **75**, 559
 Perlmutter S., et al., 1999, *ApJ*, **517**, 565
 Planck Collaboration XIII 2016, *A&A*, **594**, A13
 Riess A. G., et al., 1998, *AJ*, **116**, 1009
 Ruiz E. J., Huterer D., 2015, *Phys. Rev. D*, **91**, 063009
 Sahni V., Shtanov Y., 2003, *J. Cosmology Astropart. Phys.*, **11**, 014
 Sahni V., Shafieloo A., Starobinsky A. A., 2008, *Phys. Rev. D*, **78**, 103502
 Sahni V., Shafieloo A., Starobinsky A. A., 2014, *ApJ*, **793**, L40
 Shafieloo A., 2007, *MNRAS*, **380**, 1573
 Shafieloo A., Alam U., Sahni V., Starobinsky A. A., 2006, *MNRAS*, **366**, 1081
 Shafieloo A., Kim A. G., Linder E. V., 2013, *Phys. Rev. D*, **87**, 023520
 Solà J., Gómez-Valent A., de Cruz Pérez J., 2017, *Modern Physics Letters A*, **32**, 1750054
 Song Y.-S., Percival W. J., 2009, *J. Cosmology Astropart. Phys.*, **10**, 004
 Spergel D., et al., 2015, preprint, ([arXiv:1503.03757](https://arxiv.org/abs/1503.03757))
 Weinberg S., 1989, *Reviews of Modern Physics*, **61**, 1
 Zhao G.-B., et al., 2017, *Nature Astronomy*, **1**, 627
 de Felice A., Tsujikawa S., 2010, *Living Reviews in Relativity*, **13**
 de la Torre S., Peacock J. A., 2013, *MNRAS*, **435**, 743

APPENDIX A: DATA VISUALIZATION

For visualization purpose, Fig. A1 shows some reconstructed $f\sigma_8$ verifying eq. (14) and with $\chi^2 < \chi^2_{\Lambda\text{CDM}}$.

This paper has been typeset from a T_EX/L^AT_EX file prepared by the author.